

Intrinsic local destabilization of the C-terminus predisposes integrin $\alpha 1$ I domain to a conformational switch induced by collagen binding

Ana Monica Nunes,^{1,2} Jie Zhu,^{1,2} Jacqueline Jezioro,^{1,2}
Conceição A.S.A. Minetti,¹ David P. Remeta,¹ Richard W. Farndale,³
Samir W. Hamaia,^{3*} and Jean Baum^{1,2*}

¹Department of Chemistry & Chemical Biology, Rutgers University, Piscataway, New Jersey 08854

²Center for Integrative Proteomics Research, Rutgers University, Piscataway, New Jersey 08854

³Department of Biochemistry, University of Cambridge, Cambridge CB2 1QW, United Kingdom

Received 7 June 2016; Accepted 22 June 2016

DOI: 10.1002/pro.2972

Published online 24 June 2016 proteinscience.org

Abstract: Integrin–collagen interactions play a critical role in a myriad of cellular functions that include immune response, and cell development and differentiation, yet their mechanism of binding is poorly understood. There is increasing evidence that conformational flexibility assumes a central role in the molecular mechanisms of protein–protein interactions and here we employ NMR hydrogen–deuterium exchange (HDX) experiments to explore the impact of slower timescale dynamic events. To gain insight into the mechanisms underlying collagen-induced conformational switches, we have undertaken a comparative study between the wild type integrin $\alpha 1$ I and a gain-of-function E317A mutant. NMR HDX results suggest a relationship between regions exhibiting a reduced local stability in the unbound I domain and those that undergo significant conformational changes upon binding. Specifically, the αC and $\alpha 7$ helices within the C-terminus are at the center of such major perturbations and present reduced local stabilities in the unbound state relative to other structural elements. Complementary isothermal titration calorimetry experiments have been performed to derive complete thermodynamic binding profiles for association of the collagen-like triple-helical peptide with wild type $\alpha 1$ I and E317A mutant. The differential energetics observed for E317A are consistent with the HDX experiments and support a model in which intrinsically destabilized regions predispose

Abbreviations: $\alpha 1$ I, alpha1 I domain; NMR, nuclear magnetic resonance; HDX, hydrogen–deuterium exchange; HSCQ, hetero-nuclear single-quantum correlation; MIDAS, metal ion-dependent adhesion site; THP, collagen-like triple helical peptide; ITC, isothermal titration calorimetry; CD, circular dichroism.

Additional Supporting Information may be found in the online version of this article.

Integrin–collagen interactions play a critical role in cell adhesion processes. To gain insight into the mechanisms underlying collagen-induced conformational switches, we have undertaken a comparative NMR study between the human integrin $\alpha 1$ I and a gain-of-function E317A mutant. Our results, supported by thermodynamic measurements, suggest that intrinsically destabilized regions facilitate conformational rearrangements of integrin I domain. This study highlights the importance of exploring slow dynamics to delineate allosteric and binding events.

Grant sponsor: National Institutes of Health; Grant number: GM45302 (JB); Grant sponsor: American Heart Association postdoctoral fellowship; Grant number: 13POST16550007 (AMN); Grant sponsor: Wellcome Trust Biomedical Resource; Grant number: 094470/Z/10/Z (RWF).

*Correspondence to: Jean Baum, Department of Chemistry & Chemical Biology, Rutgers University, 610 Taylor Road, Piscataway, New Jersey 08854. E-mail: baum@chem.rutgers.edu; Samir W. Hamaia, Department of Biochemistry, University of Cambridge, Cambridge CB2 1QW, United Kingdom. E-mail: swh23@cam.ac.uk

conformational rearrangement in the integrin I domain. This study highlights the importance of exploring different timescales to delineate allosteric and binding events.

Keywords: NMR; $\alpha 1 \beta 1$ I domain; integrin; collagen; hydrogen–deuterium exchange; conformational switch; dynamics; binding energetics

Introduction

Collagen interactions with $\alpha 1 \beta 1$ integrin receptors play a key role in numerous cellular processes, spanning cell development to differentiation and hemostasis to immune responses.^{1–3} Integrin $\alpha 1 \beta 1$ is widely expressed in mesenchyme cells, the immune system, and a minority of epithelial tissues.³ Functionally, $\alpha 1$ is one of four collagen binding I domains containing $\beta 1$ partners that includes $\alpha 2$, $\alpha 10$, and $\alpha 11$. Upon binding to a collagen peptide, the I domain of integrin $\alpha 1 \beta 1$ ($\alpha 1$ I) undergoes conformational changes^{4–7} similar to those observed in the $\alpha 2$ I domain,^{4–7} in which coordination of a collagen glutamate to the metal ion-dependent adhesion site (MIDAS) at the top of $\alpha 1$ I induces a shift from the “closed” (unliganded) to “open” (liganded) conformation. This switch induces allosteric changes in the C-terminus of the Rossmann-fold structure, with helix αC unfolding and helix $\alpha 7$ displacing 12 Å downwards. The resultant movement permits coordination to a second allosteric site within helix $\alpha 7$ to the β -subunit and propagates these structural changes throughout the entire integrin macromolecule.¹

Despite the critical functional importance of collagen–integrin interactions *in vivo*, the mechanism of integrin binding to collagen requires elaboration at the structural, dynamic, and thermodynamic levels. In an attempt to gain mechanistic insights into the I domain activation process induced by collagen, several “gain-of-function” mutants that result in enhanced binding to collagen have been studied.^{8–12} Specifically, the $\alpha 1$ I mutant E317A has been characterized by high resolution X-ray crystallography¹³ and numerous binding assays report an increase of binding to collagen.^{11,13} The residue E317 is located at the top of helix $\alpha 7$ and is linked to helix αC (R287) via a salt bridge, a stabilizing feature of the closed unliganded form. The E317A mutation eliminates this salt bridge and adopts a transition state between the $\alpha 1$ I closed-unbound form and the open-bound form. Indeed, an X-ray structure of the E317A mutant has revealed a novel conformation in which helix $\alpha 7$ is in the closed upward position, helix αC is unstructured (as observed in the open-bound form), and the metal ion is reported as adopting a unique penta-coordination.¹³ Although the gain in function is primarily ascribed to structural changes that are implicated in reducing the ligand binding barrier relative to wild type protein, dynamics must be considered when describing the mechanism by which a gain of activity occurs.

There is increasing evidence that conformational flexibility assumes a central role in the molecular mechanisms of protein–protein interactions.^{14–17} NMR is well suited for studying the conformation and dynamics of proteins and can provide information over a broad spectrum of timescales ranging from picoseconds to seconds and hours.^{14,15} Conformational fluctuations on the micro to millisecond timescales have been shown to be critical determinants of biological processes in protein recognition and allosteric events.^{14–18} In this study, we explore the role of slower timescale dynamic events that occur in the unbound free protein to unravel specific mechanisms that precede collagen binding. Hydrogen–deuterium exchange (HDX) kinetics measured via NMR affords the advantage of characterizing slow conformational fluctuations in denaturant free environments and thereby provides site-specific information on local stability in the native state.^{19–23}

In the current investigation, NMR HDX experiments demonstrate the importance of slow motions in terms of predisposing integrin to conformational changes upon binding. Our NMR HDX results suggest a relationship between regions exhibiting a reduced local stability in the unbound I domain and those that undergo significant conformational changes upon binding. The αC and $\alpha 7$ helices of $\alpha 1$ I are at the center of such major perturbations and have reduced local stabilities in the unbound state, relative to other structural elements. Significantly, a combined energetic and structural characterization suggests that E317A activation and enhancement of collagen binding affinity are primarily dynamic in origin. The latter includes intermediary timescale motions in helix αC and MIDAS, as well as propagation of slow conformational fluctuations to additional structural elements within the C-terminus. Our findings underscore the relevance of slow conformational dynamics, intrinsic to the free $\alpha 1$ I, and the concomitant reduction of local stability within regions of a conformational switch. The latter assumes a critical role in allosteric regulation presumably by decreasing the overall energetic penalty associated with ligand-binding interactions.

Results

HDX NMR experiments reveal conformational fluctuations in the I domain of human $\alpha 1 \beta 1$ integrin
HDX measurements of $\alpha 1$ I integrin provide detailed information regarding conformational fluctuations

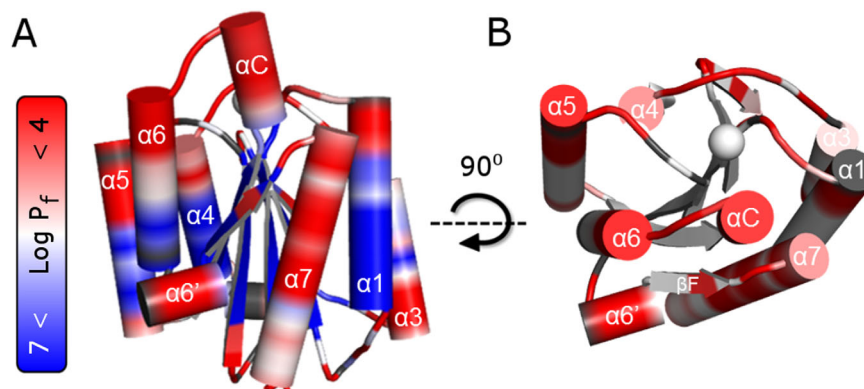


Figure 1. Hydrogen–deuterium exchange of $\alpha 1$ I integrin. The logarithmic value of protection factors (P_f) obtained from the HDX exchange rates, are mapped in the representation of **(A)** wild type $\alpha 1$ I (PDB #1pt6) in the closed-unbound form. The residues that do not exchange with solvent for over two months exhibit high P_f ($\text{Log } P_f > 7$) and are colored in blue, whereas residues that are highly dynamic (i.e., exchange with solvent so fast that these disappear from the NMR spectra after 20 min) exhibit reduced P_f ($\text{Log } P_f < 4$) and are colored in red (refer to color bar). **(B)** Top view highlighting the flexibility of residues located at the top of collagen binding site in $\alpha 1$ I. Note that the blue color is removed for ease of visualization. Unassigned or overlapped peaks are colored in gray and the metal is represented as a sphere.

based on the amide NH protection factors (P_f).^{19,23} Well-dispersed resonances in the [^1H - ^{15}N]-TROSY spectrum (Supporting Information Figs. S1A and S4A) are characteristic of a well-folded protein.⁶ HDX measurements for 186 non-overlapping residues in $\alpha 1$ I reveal 32% fast-exchanging amide protons with low P_f , and 23% slowly exchanging residues with high P_f [Fig. 1(A)]. The remaining 45% exhibit a time-dependent decrease in peak intensity and their observed exchange rate constants (k_{obs}), P_f , and free exchange energies (ΔG_{HX}) are summarized in Supporting Information Table SI.

There are four major observations that can be deduced from the HDX kinetics data of $\alpha 1$ I [Fig. 1(A), Supporting Information Table SI]. First, $\alpha 1$ I contains a highly protected β -sheet core with amide protons that exhibit P_f values of 10^6 – 10^7 [$\text{Log } P_f = 6$ – 7 in Fig. 1(A)] comparable in magnitude to those observed for typical 10–20 kDa proteins.^{24,25} Second, residues located in the upper face possess lower P_f values with faster HDX exchange rates than residues in the lower face [Fig. 1(B)]. Most of these fast-exchanging residues comprise unstructured loops and α -helical structures with the exception of helix $\alpha 3$. Third, highly protected loops of $\alpha 3$ - βC and $\alpha 6$ - βF are located in the bottom face (P_f of 10^5 – 10^6 compared to 10^2 – 10^4 in other loops), consistent with the existence of a hydrophobic intramolecular pocket observed in other I domains.^{26–29} Fourth, fast HDX rates are observed in helices αC and $\alpha 7$. Indeed, these residues present remarkably low P_f values for a helical conformation (10^4 – 10^5). In fact, only G283 in helix αC (G²⁸³SYNR²⁸⁷) exhibit measurable P_f values on the order of 10^5 . These two helices are known to undergo a major structural rearrangement upon complexation [Fig. 2(A)].^{7,30} Thus, the data suggest a relationship between fast

HDX rates in the unbound $\alpha 1$ I and residues that undergo significant conformational change upon complexation. HDX can be interpreted in terms of the free exchange energies or local stability (ΔG_{HX}) by assuming an EX2 limit,³¹ whereby the conformational equilibrium between unfolded and folded states is much faster than the intrinsic exchange rate. HDX will be discussed within the context of local stability (ΔG_{HX}) in subsequent sections of this manuscript.

Low local stabilities derived from HDX experiments can arise from increased solvent accessibility. We have therefore investigated the relationship between local stabilities derived from HDX experiments, solvent accessible surface areas (SASA), and conformational changes in the $\alpha 1$ I structure ($\Delta r\text{C}\alpha$) induced by collagen binding [Fig. 2(B)]. High $\Delta r\text{C}\alpha$ values correspond to large conformational differences between the unbound-closed and bound-open forms of $\alpha 1$ I. In the overlay of both $\alpha 1$ I forms (Fig. 2), helix $\alpha 7$ translocates Å downward upon ligand binding and helix αC becomes an unstructured loop.⁷ Solvent accessible surface areas (SASA) derived from analysis of the three-dimensional structures measure solvent accessibility to an amide within the protein. Residues characterized by large SASA values are highly accessible to solvent and usually exhibit low P_f values (e.g., loops), while residues with low SASA values are buried from solvent. The most striking feature illustrated in this figure is the presence of residues (highlighted by drop lines) with low SASA that present low P_f values represented by reduced local stabilities (ΔG_{HX}), all of which correspond to residues with the highest displacement (high $\Delta r\text{C}\alpha$). These residues are confined to the C-terminus of $\alpha 1$ I [Fig. 2(B)] and are primarily located in helices αC and $\alpha 7$.

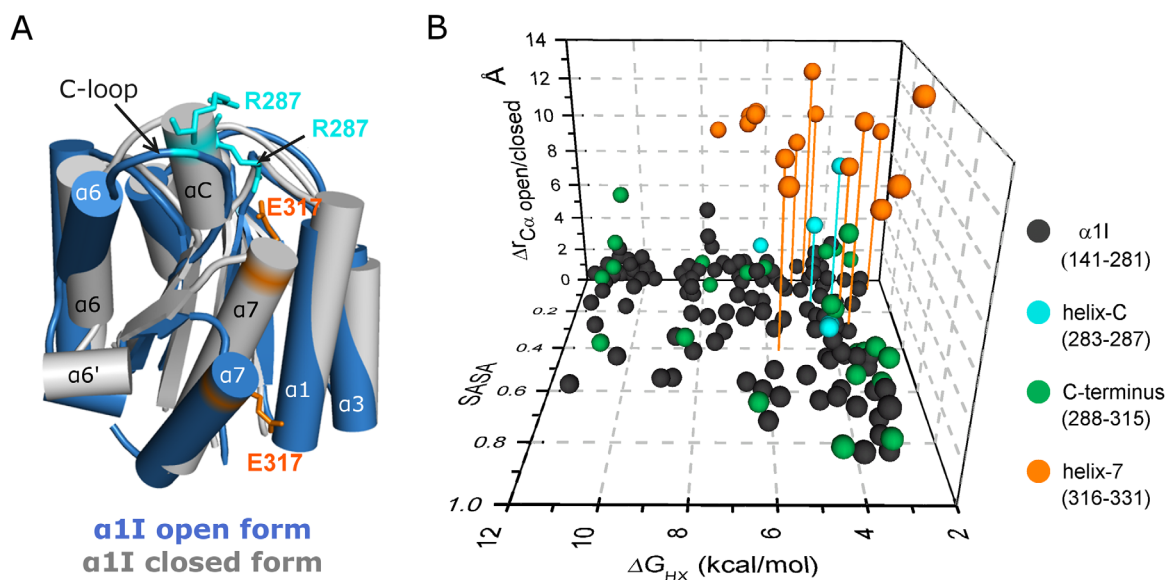


Figure 2. Relationship between conformational change upon complexation for $\alpha 1$ I residues, local stability, and solvent accessibility (SASA). (A) The X-ray $\alpha 1$ I closed-unbound structure (gray, PDB #1pt6) is overlaid with the first conformer of the GLO-GEN bound open $\alpha 1$ I NMR structure (blue, PDB #2m32). The stick representation of E317 (orange) and R287 (cyan) residues highlight their distinct positions before and after collagen binding. (B) Correlation between $\alpha 1$ I free energy of exchange (ΔG_{HX}) obtained from the protection factors, solvent accessible surface area (SASA), and distance between the alpha-carbon ($\Delta rC_{\alpha \text{ open/closed form}}$) in the closed and open structures of $\alpha 1$ I taken from the X-ray⁶ and NMR⁷ structures. The C-terminal residues are colored in green except for residues assigned to helix-7 (orange) and C-helix (cyan). Drop lines highlight residues that have $\Delta rC_{\alpha} > 5 \text{ \AA}$, $\Delta G_{HX} < 6 \text{ kcal/mol}$ and $SASA < 0.5$. Helices that have unusually low local stabilities (i.e., αC and $\alpha 7$ helices in the closed form) undergo large structural changes upon binding to GLO-GEN.

Activated E317A $\alpha 1$ I mutant is more dynamic than its wild type counterpart

Our NMR data, using an E317A/ $\alpha 1$ I sequence construct that is similar to the X-ray study, reveals 90% of the expected resonances (independent of the experimental conditions). The majority of missing resonances correspond to residues located in the L1 and L3 loops of MIDAS and helix αC and are attributed to conformational exchange dynamics on the micro-millisecond timescale (Supporting Information Figs. S1B and S1C). For the resonances that are observed, ^{13}C chemical shift analysis³² suggests that E317A/ $\alpha 1$ I retains a secondary structure in solution which is identical to the crystal structure¹³ (Supporting Information Fig. S1B) with the exception of helix αC and the MIDAS loops for which the NMR resonances are missing. Chemical shift difference spectra between E317A and the wild type protein support the notion that helix $\alpha 7$ is positioned upward as it is in the closed state (Supporting Information Fig. S1C). These results do not agree with previous NMR studies^{7,33} that reported $\alpha 7$ in a downward position as in the open-bound form. This discrepancy may arise from the absence of reported peak assignments or from a different protein construct used in previous NMR studies relative to the crystal structure¹³ and our present NMR studies. The Scanlon group uses a construct exhibiting a truncation of the last three residues in helix $\alpha 7$ with the sequence terminating at I331.⁷

E317A/ $\alpha 1$ I HDX experiments indicate that 31 and 20% of the residues are in fast and slow exchange, respectively and explicit kinetic parameters have been determined for 34% of these residues (Supporting Information Table SI). Comparison of the HDX parameters for E317A/ $\alpha 1$ I and $\alpha 1$ I [Figs. 1(A) and 3(A)] indicate similar tendencies overall to those observed for $\alpha 1$ I; however, there are local regions in E317A that exhibit a decrease in P_f values. A more quantitative comparison of ΔG_{HX} reveals that the HDX of the beta-sheet core residues in $\alpha 1$ I and E317A do not change appreciably, yet regions important for conformational rearrangement from the closed to open form exhibit both a lower average and narrower distribution of ΔG_{HX} [Fig. 3(B)]. This is particularly significant in helix $\alpha 6$, strand βF , and helix $\alpha 7$, with the activating mutant in helix $\alpha 7$ exhibiting a lower and narrower distribution of ΔG_{HX} . Indeed, the C-terminus secondary-structure elements present an overall destabilization of $5.6 \text{ kcal}\cdot\text{mol}^{-1}$ relative to wild type $\alpha 1$ I. The βF -strand ΔG_{HX} median value is $4.0 \text{ kcal}\cdot\text{mol}^{-1}$ less stable in the mutant, while helices $\alpha 6$ and $\alpha 7$ are destabilized by 0.7 and $0.9 \text{ kcal}\cdot\text{mol}^{-1}$, respectively.

Energetics of wild type $\alpha 1$ I and E317A interactions with a collagen model peptide

Full-length collagen sequences contain multiple binding sites exhibiting variable integrin affinities^{9,34,35} that effectively precludes an accurate

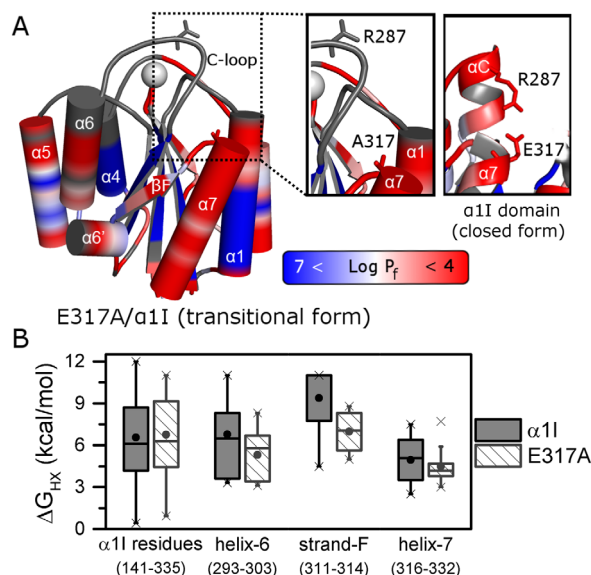


Figure 3. Hydrogen–deuterium exchange of $\alpha 1$ I activating mutant, E317A. (A) The logarithmic value of protection factors ($\text{Log } P_f$, refer to color bar) is mapped onto the crystal structure of the activated E317A/ $\alpha 1$ I (PDB #4a0q) mutant. Unassigned or overlapped peaks are colored in gray, and the metal is represented as a sphere. A close-up of E317 and R287 residues comprising the salt-bridge in the wild type (right panel) appears on the left for E317A. (B) Boxplot diagram representing the dispersion of local free energy of exchange for amide protons (ΔG_{HX}) of $\alpha 1$ I wild type (gray) and E317A (hatch white). This box represents the statistical distribution between 25% and 75% of the full sequence and the C-terminus with helices $\alpha 6$, $\alpha 7$, and βF strand plotted separately. The mean value is depicted by a ball and the whiskers represent maximum/minimum values of all data.

energetic characterization. Synthetic collagen-like triple-helical peptides (THP) represent a suitable model for biophysical^{5,7,30,36–39} and functional studies^{9,34,35} of collagen. In an effort to elucidate the forces that promote $\alpha 1$ I binding to collagen and the origins of E317A enhanced activity observed in adhesion assays toward collagens I and IV (Supporting Information Fig. S2), we have employed ITC to derive complete thermodynamic binding profiles for association of Ac-(GPO)₄GLOGEN(GPO)₄GY-NH₂ (GLOGEN) THP with wild type $\alpha 1$ I and the E317A mutant (Supporting Information Fig. S3). We specifically selected this high affinity GLOGEN binding sequence³⁵ to provide structural, dynamic, and thermodynamic insight on the $\alpha 1$ I-collagen interaction.

Association of both I-domains with THP is characterized by formation of a 1:1 stoichiometric complex with favorable enthalpic and entropic contributions

(Table I). The Gibbs free energy of $-5.98 \text{ kcal}\cdot\text{mol}^{-1}$ determined for the $\alpha 1$ I-GLOGEN interaction yields a dissociation constant of $\sim 20 \text{ }\mu\text{M}$ that corroborates solid phase binding studies.³⁵ While wild type interactions are predominantly entropy-driven, peptide association with the mutant is characterized by nearly identical enthalpic and entropic components. The E317A activation of $\alpha 1$ I is accompanied by an approximately threefold enhancement in binding affinity, which is the result of a more favorable enthalpy (i.e., $\Delta\Delta H = -1.88 \text{ kcal}\cdot\text{mol}^{-1}$) and a concomitant loss in entropy (i.e., $\Delta T\Delta S = -1.32 \text{ kcal}\cdot\text{mol}^{-1}$). This characteristic enthalpy–entropy compensation yields a small net gain in the overall Gibbs binding free energy ($\Delta\Delta G$) of $-0.56 \text{ kcal}\cdot\text{mol}^{-1}$. Direct HDX characterization by NMR of the wild type $\alpha 1$ I-GLOGEN complex is not possible as the $20 \text{ }\mu\text{M}$ dissociation constant determined for $\alpha 1$ I-GLOGEN interaction positions the interconversion between bound–unbound forms in an intermediate timescale, which results in resonance broadening within the NMR spectra of the complex (refer to Supporting Information Fig. S4). Nevertheless, the regions of $\alpha 1$ I most broadened by the addition of GLOGEN include the binding interface (particularly MIDAS, Supporting Information Fig. S4C,D) and the regions of structural rearrangement (primarily the C-terminus, Supporting Information Fig. S4C,E).

Discussion

The mechanisms that regulate $\alpha 1$ I ligand affinity of integrin and its intrinsic ability to undergo structural rearrangements upon binding to the rigid rod-shaped collagen remain unclear. Conformational fluctuations have been proposed as a driving force for several binding and allosteric events.^{14–17} The majority of these studies have focused on dynamic fluctuations occurring on the micro- to millisecond timescale^{14,18,40} in contrast to the impact of slower timescales on conformational changes. Much of what is known about allosteric activation of integrins caused by collagen binding has been derived from structural studies of both $\alpha 1$ and $\alpha 2$ I domains.^{5–7,13,41} These studies have captured static conformational “snapshots” of the collagen binding $\alpha 1$ I in three different conformations: a closed-unbound structure determined by X-ray,^{6,41} a transitional conformation adopted by the gain-of-function E317A/ $\alpha 1$ I mutant determined by X-ray,¹³ and an open-bound form determined by solution NMR with a complexed GLOGEN THP.⁷ The first glimpse of $\alpha 1$

Table I. Thermodynamic binding parameters derived from calorimetric measurements of the wild type and activating mutant E317A/ $\alpha 1$ I titrated into GLOGEN at 5.0°C

Integrin	K_d (μM)	K_a 10^5 (M^{-1})	ΔG ($\text{kcal}\cdot\text{mol}^{-1}$)	ΔH ($\text{kcal}\cdot\text{mol}^{-1}$)	$T\Delta S$ ($\text{kcal}\cdot\text{mol}^{-1}$)
Wild type $\alpha 1$ I	19.9 ± 0.50	0.50 ± 0.01	-5.98 ± 0.15	-1.32 ± 0.02	$+4.66 \pm 0.10$
E317A/$\alpha 1$ I	7.25 ± 0.13	1.38 ± 0.02	-6.54 ± 0.02	-3.20 ± 0.02	$+3.34 \pm 0.05$

I slow dynamics originated from a HDX mass spectroscopy study on a $\alpha 1$ I rat-human chimera and provided important insights on the impact of different ligands on integrin activation.⁴² To assess the role of intrinsic conformational fluctuations on the structural switch, our studies focus on elucidating the dynamics of unbound human $\alpha 1$ I integrin and its activating E317A mutant at the atomic level by HDX NMR spectroscopy in combination with ITC to evaluate the binding energetics. The resultant data suggest that slow timescale motions may be an integral determinant of α I-domain propensity to undergo significant structural changes upon collagen binding.

Intrinsic local destabilization of $\alpha 1$ I in the unbound-closed form facilitates a conformational switch to the open form

The difference in local stability as seen by HDX experiments between the upper and bottom face of the $\alpha 1$ I is quite significant, with the region that binds collagen,^{7,42} at the top of $\alpha 1$ I, undergoing much faster exchange rates [Fig. 1(B)]. We propose that this increase in plasticity of the collagen binding interface might be required to allow the globular I domain to incorporate the rigid rod-like shape of the collagen structure. These slow timescale motions probed by HDX experiments are important for collagen recognition mechanisms in matrix metalloproteinases³⁷ and may thereby assist in optimizing $\alpha 1$ I-collagen interactions.

The unusually low local stability of αC and $\alpha 7$ in wild type $\alpha 1$ I reveals that these helices undergo a local breathing or accordion-like motion. Notably, these helices are at the center of major structural rearrangements in the conformational switch of $\alpha 1$ I. In the complex, helix αC becomes unfolded and helix $\alpha 7$ exhibits a major displacement of 12 Å. The highly dynamic character of helix $\alpha 7$ is consistent with NMR and molecular dynamics studies of other I domain integrins.^{43–46} The data suggest a correlation between residues prone for allosteric movement and reduced local stability despite low solvent accessibility. We hypothesize that local destabilization of structural elements in the unbound I domain facilitates the conformational rearrangement induced by collagen.

Enhanced dynamics of unbound E317A/ $\alpha 1$ I contributes to gain of functionality

To test our hypothesis we used an activated mutant of $\alpha 1$ I, E317A, that has been characterized by X-ray crystallography¹³ and affinity assays.^{11,13} It provides mechanistic insight into the $\alpha 1$ I activation process due to its increase of affinity toward collagen and its transitional conformation.¹³ Here, we hypothesize that the increased binding affinity is also the result

of higher local destabilization of the regions of conformational rearrangement.

NMR HDX measurements described in this study reveal that the E317A dynamics are more complex than wild type $\alpha 1$ I, particularly in the region of αC and MIDAS loops. Helix αC is a unique structural element of collagen-binding integrins that is proposed to be a determinant of selectivity for collagen^{5,47,48} by functioning via steric hindrance.¹¹ In wild type $\alpha 1$ I, NMR resonances are observed for helix αC , whereas the latter are not detected in E317A. Signal loss provides valuable dynamic information, as peak broadening observed within the activating mutant indicates that helix αC and MIDAS loops are in conformational exchange.^{14,18} In addition, the absence of peaks for helix αC , rather than the existence of sharp resonances expected for unfolded regions, implies that these residues are in intermediate exchange on the NMR timescale rather than fully unfolded as observed in the X-ray structure (Fig. 2). The E317A chemical shifts surrounding the MIDAS loops (refer to Supporting Information Fig. S1C) support a chemical environment that is distinct from wild type $\alpha 1$ I. Thus, we propose that the conformation of helix αC and MIDAS loops are in conformational exchange in solution, and that helix αC may be interconverting between folded-unfolded conformations on a fast micro-second to millisecond timescale, reducing the steric hindrance to collagen.

On the slower timescale motions, our HDX results on the activating mutant E317A/ $\alpha 1$ I reveal a propagation of the trends already observed in wild type $\alpha 1$ I, and reflect an even lower and narrower range of local stabilities for the C-terminus residues involved in allosteric movement. The slow conformational dynamics are propagated from helix $\alpha 7$ to helix $\alpha 6$ and strand βF in the gain-of-function mutant, disturbing to a higher degree (than in wild type $\alpha 1$ I) the contacts within the hydrophobic intramolecular pocket.^{26–29} Indeed, destabilization of the hydrophobic core has been linked with an increase of binding toward collagen.^{28,49} Moreover, deletion of three residues within helix $\alpha 7$ enhances the binding of $\alpha 1$ I to GLOGEN and allows visualization of the complex by NMR (refer to Supporting Information Fig. S4C).⁷ Higher destabilization of the E317A C-terminus coupled with the increase in binding affinity supports the hypothesis that these slow transient fluctuations observed in the unbound E317A/ $\alpha 1$ I contribute to the gain-of-function by facilitating conformational rearrangement.

Thermodynamic basis of integrin-collagen interactions

Further corroboration of the forces driving association of $\alpha 1$ I with the THP may be deduced via comparisons of the respective thermodynamic profiles

for both wild type $\alpha 1$ I and E317A mutant (refer to Table I). The E317A mutant exhibits approximately a three-fold increase in affinity relative to wild type $\alpha 1$ I. The net enthalpic improvement of E317A association (i.e., $\Delta\Delta H = -1.9$ kcal·mol⁻¹) compared to its wild type counterpart presumably results from abrogation of an unfavorable enthalpy that arises from local unfolding of the αC helix, and salt-bridge disruption that occurs upon collagen binding to the wild type. We suggest that hydrogen bonds are more transient in E317A due to absence of the salt bridge, faster dynamics of the αC helix and MIDAS loops, and the more destabilized C-terminus. Collectively, our findings on the E317A mutant suggest that the unbound form populates an ensemble of states that are conformationally more suited to ligand association, thereby reducing the overall energy (enthalpy) penalty imposed by major structural changes that must occur in the wild type.

Conclusions

Elucidating the forces that drive allostery is critical to understanding the complex transformations of biomolecules. The unique heterogeneous shape of a rod-like extracellular matrix protein associated with a globular cellular receptor prompts us to explore new timescales. HDX experiments on the wild type and activated α subunit I domains of integrin suggest that collagen binding and the induced conformational change are facilitated by destabilization of the C-terminus secondary-structure elements and residues comprising the integrin–collagen interface. Nature designed this domain with regions prone for conformational rearrangement given their inherent dynamics and intrinsic destabilization. Collectively, our characterization of slow dynamics in the integrin $\alpha 1$ I domain and the underlying binding energetics provides an instructive example on the relationship between local destabilization and propensity for allosteric structural changes. In an era where NMR microsecond timescale motions are critical for elucidating allosteric mechanisms, this study highlights the importance of exploring different timescales as part of a comprehensive experimental strategy to delineate allosteric and binding events.

Materials and Methods

I domains expression and purification

The recombinant $\alpha 1$ I from human integrin $\alpha 1\beta 1$ used for these studies corresponds to residues T141–E335. Protein purification was conducted as previously described,¹² but cells were grown in M9 media supplemented with ¹⁵NH₄Cl₂, and [¹³C₆]-D-glucose and deuterated water was used when required to obtain isotopically ²H, ¹³C, ¹⁵N labeled proteins. Protein concentration was determined via measurement

of the absorption at 280 nm employing the respective molar extinction coefficients.

NMR spectroscopy

Spectra were acquired on a 700-MHz Bruker spectrometer equipped with a cryoprobe. For experimental details refer to Supporting Information. Triple resonance experiments allowed assignments of 98 and 90% of the complete backbone resonances (195 residues) for wild type $\alpha 1$ I and E317A/ $\alpha 1$ I, respectively, and agree with previous NMR studies of wild type $\alpha 1$ I.⁵⁰ Chemical shifts of all assigned resonances of E317A/ $\alpha 1$ I were deposited in the BMRB under accession number 26822. TALOS+⁵¹ was used to estimate the secondary structure in solution based on the ¹³C resonances. The analysis of ¹³C $^{\alpha}$, ¹³C $^{\beta}$, ¹³CO resonances³² reveals a comparable $\alpha 1$ I and E317A/ $\alpha 1$ I secondary structure as in the crystal structures.^{6,13,41,52} The chemical shift perturbation ($\Delta\delta$) of the backbone amides caused by mutation of E317A/ $\alpha 1$ I relative to wild type $\alpha 1$ I was calculated by the equation: $\Delta\delta = \sqrt{((0.154\Delta N^2) + \Delta H^2)/2}$ where ΔN and ΔH correspond the chemical shifts difference between the E317A's and the wild type's $\alpha 1$ I amide nitrogens and protons, respectively.⁵³ All spectra were processed using nmr-Pipe⁵⁴ and Sparky.⁵⁵

Hydrogen–deuterium exchange (HDX)

The amide exchange experiments were performed at 20°C for the ¹⁵N- $\alpha 1$ I sample with a pD of 7.10 and at 25°C for ¹⁵N-E317A/ $\alpha 1$ I with a pD of 7.4. Samples were lyophilized in 10 mM PIPES buffer containing 140 mM NaCl, 5 mM or 25 mM MgCl₂ and 1 mM DSS, with concentrations spanning the range 0.3–0.5 mM. A series of ¹H-¹⁵N HSQC spectra of the D₂O sample were acquired every 10 min for 24 hours, followed by several spectra of 1 hour duration up to 2 months for $\alpha 1$ I and 1 month for E317A/ $\alpha 1$ I. Considering the time required to setup and acquire the NMR spectra, the first time points for $\alpha 1$ I and E317A/ $\alpha 1$ I following resuspension in D₂O were 15, and 20 min, respectively. HDX reaction of the amide proton is generally described by a two-step model between the folded (NH_{closed}) and unfolded (NH_{open}) states versus the exchanged (NH_{exchanged}) state.³¹ The protection factor (P_f) of each amide proton was determined by a ratio of individual intrinsic rate constant (k_{int}) for the intrinsic chemical HDX reaction of the freely exposed amide group and observed rate constant of exchange (k_{obs}). The amide proton decays were monitored by plotting the peak intensities against the incubation times in order to obtain the k_{obs} .⁵⁶ Experimental uncertainties for k_{obs} were obtained from fitting errors. For residues with P_f too low or too high to be quantified under our experimental conditions, the k_{obs} values were estimated to be faster than $k_{obs} = (-\ln(0.05)/t_{min})$ s⁻¹ for the lower limit residues, where t_{min} is the first time point of

each experiment considering that more than 95% of the signal intensity change has occurred. The upper limit residues were estimated to be slower than $k_{\text{obs}} = (-\ln(0.95)/t_{\text{max}}) \text{ s}^{-1}$, where t_{max} is the time point of the last spectrum acquired. Thus, HDX kinetics were estimated to be faster than $3.0 \times 10^{-3} \text{ s}^{-1}$, and $2.3 \times 10^{-3} \text{ s}^{-1}$ for $\alpha 1$ I, and E317A/ $\alpha 1$ I, respectively. The exchange in these residues is too fast for observation in the first NMR spectrum and too slow within the time frame of the experiments, thereby retaining their initial peak intensity. In contrast, the k_{obs} value for residues that do not exchange after the last experimental point were estimated to be slower than $1 \times 10^{-8} \text{ s}^{-1}$ and $2.1 \times 10^{-7} \text{ s}^{-1}$ for $\alpha 1$ I and E317A/ $\alpha 1$ I, respectively. The k_{int} values were calculated from the amino acid sequence utilizing the methods of Bai *et al.*⁵⁷ and Connelly *et al.*⁵⁸ and the program SPHERE.^{59,60} For $\alpha 1$ I, 5% of the residues were excluded from kinetic analysis due to unreliable data caused by severe resonance overlap. The exchange free energy of the amide protons was calculated from the equation $\Delta G_{\text{HX}} = RT \ln(P_r)$, where R is the gas constant and T is the absolute temperature at which exchange was monitored. Under extreme conditions where the exchange rate is much faster than the refolding rate, ΔG_{HX} estimated on the basis of EX2 limit would be larger than the actual value. Solvent accessibility was predicted using the program ASAView⁶¹ inputting the crystal structure of the unbound I domain. $\Delta rC_{\alpha_{\text{open/closed form}}}$ was calculated by measuring the C α distance between the closed X-ray structure (PDB # 1pt6) and the averaged coordinates of each conformer of the open-bound NMR structure (PDB # 2m32).

Isothermal titration calorimetry (ITC)

Thermodynamic binding parameters for the association of Ac-(GPO)₄GLOGEN(GPO)₄GY-NH₂ collagen peptide (synthesized by Dominique Bihan at Cambridge University and LifeTein) with wild type $\alpha 1$ I and E317A/ $\alpha 1$ I were determined via isothermal titration calorimetry employing a VP-ITC (MicroCal, Northampton, MA). Protein stock solutions were dialyzed exhaustively against a buffer comprised of 5 mM PIPES, 140 mM NaCl, and 100 mM MgCl₂ (pH = 7.3). The standard solutions were filtered using a 0.22 μm pore size membrane, and thoroughly degassed for 10 min. The calorimetric sample cell (1.4 mL) was filled with a 50 μM GLOGEN standard prepared in the final protein dialysate and the titration syringe (300 μL) contained a 500 μM solution of wild type $\alpha 1$ I or E317A/ $\alpha 1$ I. Each titration experiment consisted of a 2.0 μL pre-injection followed by 30 consecutive 10.0 μL injections during which the reaction heats are monitored and integrated for 5.0 min. Binding isotherms were generated by recording the integrated heats normalized for $\alpha 1$ I

concentration versus the protein:peptide ratio. A nonlinear least squares fit of the resultant profile to a single site binding model facilitates characterization of thermodynamic parameters for the protein:peptide complex including the affinity (K_a), Gibbs free energy (ΔG), enthalpy (ΔH), entropy (ΔS), and stoichiometric ratio (n). Experimental uncertainties are expressed as fitting errors determined from least squares minimization using the Origin software program.

References

1. Luo BH, Carman CV, Springer TA (2007) Structural basis of integrin regulation and signaling. *Annu Rev Immunol* 25:619–647.
2. Barczyk M, Carracedo S, Gullberg D (2010) Integrins. *Cell Tissue Res* 339:269–280.
3. Gardner H (2014) Integrin alpha1beta1. *Adv Exp Med Biol* 819:21–39.
4. Emsley J, King SL, Bergelson JM, Liddington RC (1997) Crystal structure of the I domain from integrin alpha2beta1. *J Biol Chem* 272:28512–28517.
5. Emsley J, Knight CG, Farndale RW, Barnes MJ, Liddington RC (2000) Structural basis of collagen recognition by integrin alpha2beta1. *Cell* 101:47–56.
6. Nymalm Y, Puranen JS, Nyholm TK, Kapyla J, Kidron H, Pentikainen OT, Airene TT, Heino J, Slotte JP, Johnson MS, Salminen TA (2004) Jararhagin-derived RKKH peptides induce structural changes in alpha1I domain of human integrin alpha1beta1. *J Biol Chem* 279:7962–7970.
7. Chin YK, Headey SJ, Mohanty B, Patil R, McEwan PA, Swarbrick JD, Mulhern TD, Emsley J, Simpson JS, Scanlon MJ (2013) The structure of integrin alpha1I domain in complex with a collagen mimetic peptide. *J Biol Chem* 288:36796–36809.
8. Aquilina A, Korda M, Bergelson JM, Humphries MJ, Farndale RW, Tuckwell D (2002) A novel gain-of-function mutation of the integrin alpha2 VWFA domain. *Eur J Biochem* 269:1136–1144.
9. Siljander PR, Hamaia S, Peachey AR, Slatter DA, Smethurst PA, Ouwehand WH, Knight CG, Farndale RW (2004) Integrin activation state determines selectivity for novel recognition sites in fibrillar collagens. *J Biol Chem* 279:47763–47772.
10. Raynal N, Hamaia SW, Siljander PR, Maddox B, Peachey AR, Fernandez R, Foley LJ, Slatter DA, Jarvis GE, Farndale RW (2006) Use of synthetic peptides to locate novel integrin alpha2beta1-binding motifs in human collagen III. *J Biol Chem* 281:3821–3831.
11. Tulla M, Lahti M, Puranen JS, Brandt AM, Kapyla J, Domogatskaya A, Salminen TA, Tryggvason K, Johnson MS, Heino J (2008) Effects of conformational activation of integrin alpha 1I and alpha 2I domains on selective recognition of laminin and collagen subtypes. *Exp Cell Res* 314:1734–1743.
12. Carafoli F, Hamaia SW, Bihan D, Hohenester E, Farndale RW (2013) An activating mutation reveals a second binding mode of the integrin alpha2 I domain to the GFOGER motif in collagens. *PLoS One* 8: e69833.
13. Lahti M, Bligt E, Niskanen H, Parkash V, Brandt AM, Jokinen J, Patrikainen P, Kapyla J, Heino J, Salminen TA (2011) Structure of collagen receptor integrin alpha1I domain carrying the activating mutation E317A. *J Biol Chem* 286:43343–43351.

14. Tzeng SR, Kalodimos CG (2011) Protein dynamics and allostery: an NMR view. *Curr Opin Struct Biol* 21: 62–67.
15. Palmer AG 3rd (2015) Enzyme dynamics from NMR spectroscopy. *Acc Chem Res* 48:457–465.
16. Kay LE (2016) New views of functionally dynamic proteins by solution NMR spectroscopy. *J Mol Biol* 428: 323–331.
17. Lisi GP, Loria JP (2016) Solution NMR spectroscopy for the study of enzyme allostery. *Chem Rev* 116:6323–6369.
18. Nussinov R, Ma B, Tsai CJ (2013) Multiple conformational selection and induced fit events take place in allosteric propagation. *Biophys Chem* 186:22–30.
19. Englander SW, Mayne L (1992) Protein folding studied using hydrogen-exchange labeling and two-dimensional NMR. *Ann Rev Biophys Biomol Struct* 21:243–265.
20. Bai Y, Englander SW (1994) Hydrogen bond strength and beta-sheet propensities: the role of a side chain blocking effect. *Proteins* 18:262–266.
21. Berjanskii M, Wishart DS (2006) NMR: prediction of protein flexibility. *Nat Protoc* 1:683–688.
22. Mittermaier AK, Kay LE (2009) Observing biological dynamics at atomic resolution using NMR. *Trends Biochem Sci* 34:601–611.
23. Skinner JJ, Lim WK, Bedard S, Black BE, Englander SW (2012) Protein dynamics viewed by hydrogen exchange. *Protein Sci* 21:996–1005.
24. Huyghues-Despointes BM, Scholtz JM, Pace CN (1999) Protein conformational stabilities can be determined from hydrogen exchange rates. *Nat Struct Biol* 6:910–912.
25. Huyghues-Despointes BM, Pace CN, Englander SW, Scholtz JM (2001) Measuring the conformational stability of a protein by hydrogen exchange. *Methods Mol Biol* 168:69–92.
26. Qu A, Leahy DJ (1995) Crystal structure of the I-domain from the CD11a/CD18 (LFA-1, alpha L beta 2) integrin. *Proc Natl Acad Sci USA* 92:10277–10281.
27. Huth JR, Olejniczak ET, Mendoza R, Liang H, Harris EA, Lupher ML, Jr., Wilson AE, Fesik SW, Staunton DE (2000) NMR and mutagenesis evidence for an I domain allosteric site that regulates lymphocyte function-associated antigen 1 ligand binding. *Proc Natl Acad Sci USA* 97:5231–5236.
28. Xiong JP, Li R, Essafi M, Stehle T, Arnaout MA (2000) An isoleucine-based allosteric switch controls affinity and shape shifting in integrin CD11b A-domain. *J Biol Chem* 275:38762–38767.
29. Valdramidou D, Humphries MJ, Mould AP (2008) Distinct roles of beta1 metal ion-dependent adhesion site (MIDAS), adjacent to MIDAS (ADMIDAS), and ligand-associated metal-binding site (LIMBS) cation-binding sites in ligand recognition by integrin alpha2beta1. *J Biol Chem* 283:32704–32714.
30. Emsley J, Knight CG, Farndale RW, Barnes MJ (2004) Structure of the integrin alpha2beta1-binding collagen peptide. *J Mol Biol* 335:1019–1028.
31. Englander SW, Mayne L, Krishna MM (2007) Protein folding and misfolding: mechanism and principles. *Q Rev Biophys* 40:287–326.
32. Wishart DS, Sykes BD (1994) The ¹³C chemical-shift index: a simple method for the identification of protein secondary structure using ¹³C chemical-shift data. *J Biomol NMR* 4:171–180.
33. Shi M, Pedchenko V, Greer BH, Van Horn WD, Santoro SA, Sanders CR, Hudson BG, Eichman BF, Zent R, Pozzi A (2012) Enhancing integrin alpha1 inserted (I) domain affinity to ligand potentiates integrin alpha1beta1-mediated down-regulation of collagen synthesis. *J Biol Chem* 287:35139–35152.
34. Farndale RW, Lisman T, Bihan D, Hamaia S, Smerling CS, Pugh N, Konitsiotis A, Leitinger B, de Groot PG, Jarvis GE, Raynal N (2008) Cell-collagen interactions: the use of peptide Toolkits to investigate collagen-receptor interactions. *Biochem Soc Trans* 36:241–250.
35. Hamaia SW, Pugh N, Raynal N, Nemoz B, Stone R, Gullberg D, Bihan D, Farndale RW (2012) Mapping of potent and specific binding motifs, GLOGEN and GVOGEA, for integrin alpha1beta1 using collagen toolkits II and III. *J Biol Chem* 287:26019–26028.
36. Li Y, Brodsky B, Baum J (2009) NMR conformational and dynamic consequences of a gly to ser substitution in an osteogenesis imperfecta collagen model peptide. *J Biol Chem* 284:20660–20667.
37. Xiao J, Addabbo RM, Lauer JL, Fields GB, Baum J (2010) Local conformation and dynamics of isoleucine in the collagenase cleavage site provide a recognition signal for matrix metalloproteinases. *J Biol Chem* 285: 34181–34190.
38. Fu I, Case DA, Baum J (2015) Dynamic water-mediated hydrogen bonding in a collagen model peptide. *Biochemistry* 54:6029–6037.
39. Xiao J, Sun X, Madhan B, Brodsky B, Baum J (2015) NMR studies demonstrate a unique AAB composition and chain register for a heterotrimeric type IV collagen model peptide containing a natural interruption site. *J Biol Chem* 290:24201–24209.
40. Popovych N, Sun S, Ebright RH, Kalodimos CG (2006) Dynamically driven protein allostery. *Nat Struct Mol Biol* 13:831–838.
41. Rich RL, Deivanayagam CC, Owens RT, Carson M, Hook A, Moore D, Symersky J, Yang VW, Narayana SV, Hook M (1999) Trench-shaped binding sites promote multiple classes of interactions between collagen and the adherence receptors, alpha(1)beta(1) integrin and *Staphylococcus aureus* cna MSCRAMM. *J Biol Chem* 274:24906–24913.
42. Weinreb PH, Li S, Gao SX, Liu T, Pepinsky RB, Caravella JA, Lee JH, Woods VL Jr (2012) Dynamic structural changes are observed upon collagen and metal ion binding to the integrin alpha1 I domain. *J Biol Chem* 287:32897–32912.
43. Legge GB, Kriwacki RW, Chung J, Hommel U, Ramage P, Case DA, Dyson HJ, Wright PE (2000) NMR solution structure of the inserted domain of human leukocyte function associated antigen-1. *J Mol Biol* 295:1251–1264.
44. Nam K, Maiorov V, Feuston B, Kearsley S (2006) Dynamic control of allosteric antagonism of leukocyte function antigen-1 and intercellular adhesion molecule-1 interaction. *Proteins* 64:376–384.
45. Zhang H, Casanovas JM, Jin M, Liu JH, Gahmberg CG, Springer TA, Wang JH (2008) An unusual allosteric mobility of the C-terminal helix of a high-affinity alphaL integrin I domain variant bound to ICAM-5. *Mol Cell* 31:432–437.
46. Leung HT, Kukic P, Camilloni C, Bemporad F, De Simone A, Aprile FA, Kumita JR, Vendruscolo M (2014) NMR characterization of the conformational fluctuations of the human lymphocyte function-associated antigen-1 I-domain. *Protein Sci* 23:1596–1606.
47. Dickeson SK, Mathis NL, Rahman M, Bergelson JM, Santoro SA (1999) Determinants of ligand binding specificity of the alpha(1)beta(1) and alpha(2)beta(1) integrins. *J Biol Chem* 274:32182–32191.

48. Kapyla J, Ivaska J, Riikonen R, Nykvist P, Pentikainen O, Johnson M, Heino J (2000) Integrin $\alpha(2)$ I domain recognizes type I and type IV collagens by different mechanisms. *J Biol Chem* 275:3348–3354.
49. Bajic G, Yatime L, Sim RB, Vorup-Jensen T, Andersen GR (2013) Structural insight on the recognition of surface-bound opsonins by the integrin I domain of complement receptor 3. *Proc Natl Acad Sci USA* 110:16426–16431.
50. Chin YK, Headey S, Mohanty B, Emsley J, Simpson JS, Scanlon MJ (2013) Assignments of human integrin α 1I domain in the apo and Mg(2+) bound states. *Biomol NMR Assign* 8:117–121.
51. Shen Y, Delaglio F, Cornilescu G, Bax A (2009) TALOS+: a hybrid method for predicting protein backbone torsion angles from NMR chemical shifts. *J Biomol NMR* 44:213–223.
52. Salminen TA, Nymalm Y, Kankare J, Kapyla J, Heino J, Johnson MS (1999) Production, crystallization and preliminary X-ray analysis of the human integrin α 1 I domain. *Acta Cryst D* 55:1365–1367.
53. Mulder FA, Schipper D, Bott R, Boelens R (1999) Altered flexibility in the substrate-binding site of related native and engineered high-alkaline *Bacillus subtilis*. *J Mol Biol* 292:111–123.
54. Delaglio F, Grzesiek S, Vuister GW, Zhu G, Pfeifer J, Bax A (1995) NMRPipe: a multidimensional spectral processing system based on UNIX pipes. *J Biomol NMR* 6:277–293.
55. Goddard TD, Kneller DG. SPARKY 3. University of California, San Francisco.
56. Molday RS, Englander SW, Kallen RG (1972) Primary structure effects on peptide group hydrogen exchange. *Biochemistry* 11:150–158.
57. Bai Y, Milne JS, Mayne L, Englander SW (1993) Primary structure effects on peptide group hydrogen exchange. *Proteins* 17:75–86.
58. Connelly GP, Bai Y, Jeng MF, Englander SW (1993) Isotope effects in peptide group hydrogen exchange. *Proteins* 17:87–92.
59. Zhang Y-Z. Protein and peptide structure and interactions studied by hydrogen exchange and NMR. *Structural Biology and Molecular Biophysics*. University of Pennsylvania, PA, USA.
60. SPHERE (<http://landing.foxchase.org/research/labs/roder/sphere/>).
61. Ahmad S, Gromiha M, Fawareh H, Sarai A (2004) ASAVIEW: database and tool for solvent accessibility representation in proteins. *BMC Bioinformatics* 5:51.